ORGANOMETALLICS

Communication

pubs.acs.org/Organometallics

Formation of a σ-alkane Complex and a Molecular Rearrangement in the Solid-State: [Rh(Cyp$_2$PCH$_2$CH$_2$PCyp$_2$)(η^2:η^2-C$_7$H$_{12}$)][BAr$^F_4$]

Alasdair I. McKay,[†,§] Tobias Krämer,[‡,§] Nicholas H. Rees,[†] Amber L. Thompson,[†] Kirsten E. Christensen,[†] Stuart A. Macgregor,*[,‡] and Andrew S. Weller*[,†]

[†]Department of Chemistry, University of Oxford, Mansfield Road, Oxford OX1 3TA, U.K.

[‡]Institute of Chemical Sciences, Heriot-Watt University, Edinburgh EH14 4AS, U.K.

Supporting Information

ABSTRACT: Addition of H_2 to the precursor [Rh(Cyp$_2$PCH$_2$CH$_2$PCyp$_2$)(η^2:η^2-C$_7$H$_8$)][BAr$^F_4$] gives the σ-alkane complex [Rh(Cyp$_2$PCH$_2$CH$_2$PCyp$_2$)(η^2:η^2-C$_7$H$_{12}$)][BAr$^F_4$] by a single-crystal to single-crystal reaction, as characterized by X-ray crystallography, SSNMR spectroscopy, and periodic DFT. An unexpected rearrangement of the {Rh(L$_2$)}$^+$ fragment is revealed.

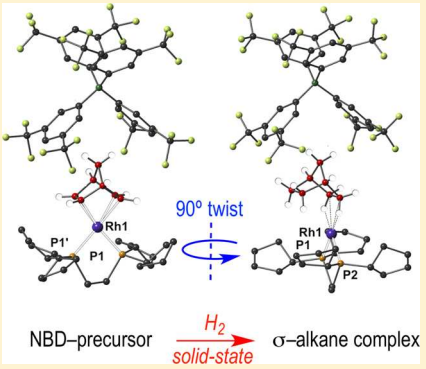

Complexes in which an alkane acts as a ligand to a metal center using its C−H bonding electrons, so-called σ-alkane complexes, are of considerable interest due to their role as intermediates in C−H activation processes and the challenges involved with their synthesis and characterization.[1] As C−H bonds are strong and non-nucleophilic, alkanes are very poor ligands, and direct observation of σ-alkane complexes has generally been limited to very low temperature in situ solution spectroscopic techniques.[2] We have recently reported that they may be prepared by solid/gas single-crystal to single-crystal transformations (Scheme 1),[3] enabling structural characterization by single crystal X-ray crystallography. Addition of H_2 to the diene precursor [Rh(R$_2$PCH$_2$CH$_2$PR$_2$)(η^2:η^2-NBD)][BAr$^F_4$] (NBD = norbornadiene, Ar^F = 3,5-(CF$_3$)$_2$C$_6$H$_3$) leads to the generation of [Rh(R$_2$PCH$_2$CH$_2$PR$_2$)(η^2:η^2-NBA)][BAr$^F_4$] (NBA = norbornane; R = ^{i}Bu, [**1-NBA**][**BAr$^F_4$**]; R = Cy, [**2-NBA**][**BAr$^F_4$**]). When R = ^{i}Bu, rapid loss of NBA in the solid-state at 298 K gives the [BAr$^F_4$]-coordinated zwitterion [**1-BAr$^F_4$**].[4] In contrast, when R = Cy, the σ-alkane complex is stable in the solid state for months at 298 K.[5] The precise factors that are responsible for these differences are currently not fully resolved. Both species feature encapsulation of the cation by an octahedral arrangement of [BAr$^F_4$]$^-$ anions, which provides a well−defined lattice environment, while the buttressing Cy groups in [**2-NBA**][**BAr$^F_4$**] may install a kinetic penalty toward rearrangement in the solid state.[4,5] We now report the synthesis of [Rh(Cyp$_2$PCH$_2$CH$_2$PCyp$_2$)(η^2:η^2-NBA)][BAr$^F_4$] using a cyclopentyl (Cyp)-substituted chelating phosphine[6] which was designed to sit between the steric profiles of flexible ^{i}Bu and rigid/tall Cy. This leads to not only a relatively stable σ-alkane complex but also an unexpected metal-fragment reorientation within the [BAr$^F_4$]$^-$ anion cavity while retaining the integrity of the single crystal.

Scheme 1. Synthesis of σ-Alkane Complexes[a]

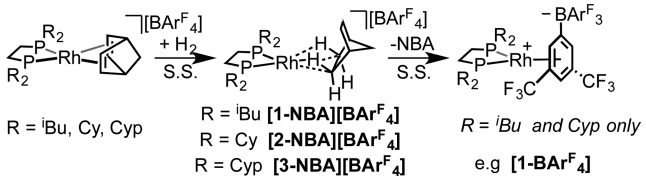

[a]S. S. = solid-state.

The precursor complex [Rh(Cyp$_2$PCH$_2$CH$_2$PCyp$_2$)(η^2:η^2-NBD)][BAr$^F_4$] ([**3-NBD**][**BAr$^F_4$**]) was prepared as for [**2-NBD**][**BAr$^F_4$**].[5] A single-crystal X-ray diffraction study at 150 K[7] (Figure 1A) demonstrated crystallographically imposed C_2 rotational symmetry with Rh1 and NBD bridge methylene (C7) occupying special positions. The Cyp groups are disordered, while the long-range structure was found to be modulated (Supporting Information),[8] which was modeled with a q vector of (0,0.3433,0).[9] The [BAr$^F_4$]$^-$ anions are organized so that each cation is contained within a pseudo-octahedral cage of anions, and the overall motif and structural

Special Issue: Hydrocarbon Chemistry: Activation and Beyond

Received: August 11, 2016
Published: September 23, 2016

DOI: 10.1021/acs.organomet.6b00645
Organometallics 2017, 36, 22−25

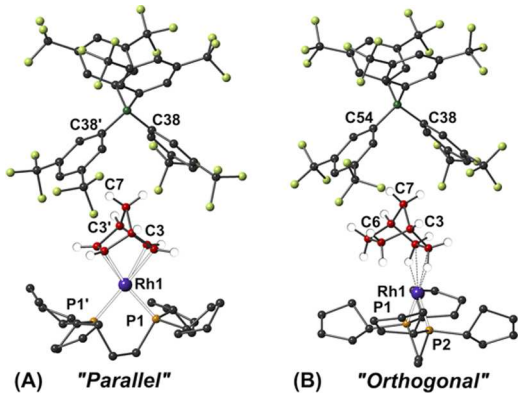

Figure 1. Solid-state structures (ball and stick) relative to a local $[BAr^F_4]^-$ anion: (A) [**3-NBA**][$\mathbf{BAr^F_4}$], average structure; (B) [**3-NBD**][$\mathbf{BAr^F_4}$]. Selected interplane angles: C38′,C38,Rh1/Rh1,P1,P1′ = 6.39(17)°; C38,C54,Rh1/Rh1,P1,P2 = 88.12(12)°.

metrics are very similar to those reported for [**2-NBD**][$\mathbf{BAr^F_4}$]. In particular the NBD ligand sits in a cleft between two $[BAr^F_4]^-$ aryl groups so that the C7-methylene protons point toward the centers of two of the aromatic rings. In the 298 K $^{31}P\{^1H\}$ solid-state NMR (SSNMR) spectrum two distinct, but very close, phosphine environments are observed (δ 66.2, J_{RhP} 149 Hz; δ 65.7, J_{RhP} 151 Hz), consistent with $PCyp_2$ disorder and/or the modulated structure. In the $^{13}C\{^1H\}$ SSNMR spectrum four signals observed between δ 90 and 55 are assigned to the NBD fragment under C_2 symmetry. The disorder/modulation was not resolved in this spectrum.

Addition of H_2 to a single-crystal sample of [**3-NBD**][$\mathbf{BAr^F_4}$] (2 bar, 10 min, 298 K) led to the quantitative formation of the σ-alkane complex $[Rh(Cyp_2PCH_2CH_2PCyp_2)(\eta^2{:}\eta^2\text{-NBA})]$-[$BAr^F_4$] ([**3-NBA**][$\mathbf{BAr^F_4}$]) (Scheme 1). Crystallinity is retained in this process, and the resulting structure determined by single-crystal X-ray diffraction (100 K, $R(2\sigma)$ = 7.0%) clearly shows a saturated NBA fragment interacting with the Rh center through two 3c-2e Rh···H−C interactions, in which the relevant hydrogen atoms were located but refined using a riding model (Figure 2). Although there are no significant changes to the arrangement of the $[BAr^F_4]^-$ anions, this

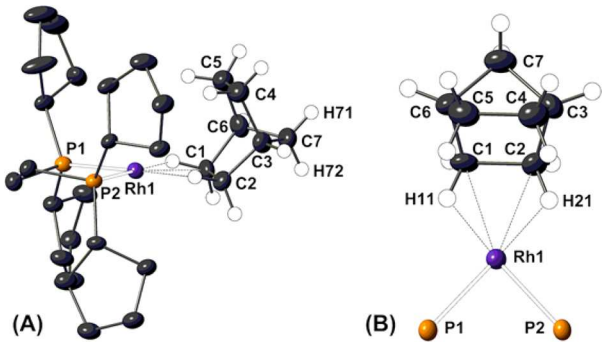

Figure 2. (A) Solid-state structure of [**3-NBA**][$\mathbf{BAr^F_4}$], with the cation and selected H atoms shown (100 K, 50% displacement ellipsoids). (B) Alternate view of [**3-NBA**][$\mathbf{BAr^F_4}$], with *P*-alkyl groups removed. Selected bond lengths (Å): Rh1−C1 2.388(5), Rh1−C2 2.392(5), Rh1−P1 2.207(1), Rh1−P2 2.206(1), C1−C2 1.550(7), C4−C5 1.541(9). Computed bond lengths (Å; periodic DFT, PBE-D3): Rh1−C1 2.425, Rh1−C2 2.420, Rh1−P1 2.219, Rh1−P2 2.215, C1−C2 1.561, C4−C5 1.565, Rh1···H11 1.895, Rh1···H21 1.886, C1−H11 1.154, C2−H21 1.154.

transformation proceeds with loss of the crystallographically imposed C_2 rotational symmetry: [**3-NBD**][$\mathbf{BAr^F_4}$], C_2/c, Z = 4; [**3-NBA**][$\mathbf{BAr^F_4}$], $P2_1/c$, Z = 4.[10] Space group changes have been noted in other single-crystal transformations.[5,11] The alkane ligand binds to the $\{Rh(L_2)\}^+$ fragment through two C−H σ-interactions, resulting in a Rh(I) square-planar, d^8 metal center coordination motif. The Rh−C1/C2 distances (2.388(5) and 2.392(5) Å, respectively) are the same, within error, as for [**2-NBA**][$\mathbf{BAr^F_4}$] (2.389(3) and 2.400(3) Å). The C1−C2 and C4−C5 distances (1.550(7) and 1.541(9) Å) signal the hydrogenation of the diene to form C−C bonds. The Rh−P distances (2.207(1) and 2.206(1) Å) are shorter than those in [**3-NBD**][$\mathbf{BAr^F_4}$] (2.2712(12) Å), reflecting the weaker trans influence C−H σ interactions. The Cyp groups showed some disorder.

The changes upon hydrogenation were also probed by the optimization of the extended solid-state structure with periodic DFT calculations at the PBE-D3 level. These provided excellent agreement both for the molecular geometries of the Rh cations (see the caption of Figure 2 for [**3-NBA**][$\mathbf{BAr^F_4}$] and the Supporting Information for [**3-NBD**][$\mathbf{BAr^F_4}$]) and for the extended structure (see Figure S15 in the Supporting Information). Moreover, the calculations provide further insight into the Rh···alkane interaction, with short average computed Rh···H11/H21 distances (1.89 Å) and elongated C1−H11 and C2−H21 distances (1.15 Å). In contrast, the C1−H12 and C2−H22 bonds exhibit standard distances of 1.10 Å, consistent with an absence of any interaction with Rh in that case. The Rh···H−C σ-interaction is confirmed by a quantum theory of atoms in molecules (QTAIM) study that identifies Rh···H11 and Rh···H21 bond paths with reduced electron densities for the C1−H11 and C2−H21 bond critical points in comparison to the C1−H12 and C2−H22 bonds.[9]

Consideration of the relationship between the cation and the proximal capping $[BAr^F_4]^-$ anion (Figure 1) shows that the NBA ligand in [**3-NBA**][$\mathbf{BAr^F_4}$] adopts an orientation very similar to that of the NBD ligand in [**3-NBD**][$\mathbf{BAr^F_4}$], in particular the orientation of the C7-methylene protons that are still directed toward the aryl rings. In contrast the $\{Rh(L_2)\}^+$ fragment has undergone a ca. 90° twist with respect to the precursor as defined by, for example, the interplane angle C38,C54,Rh1/Rh1,P1,P2 = 88.12(12)° (Figure 1). We have previously noted[12] that the octahedral cavity described by the anions accommodates a variety of structural changes associated at the metal cation. Clearly it can also accommodate significant movement of the $\{Rh(L_2)\}^+$ fragment. Whether this occurs in concert with hydrogenation, or immediately afterward, is opaque to experiment. This situation is different from that observed in the transformations that afforded [**2-NBA**][$\mathbf{BAr^F_4}$], in which it is the organic fragment that responds by moving rather than $\{Rh(L_2)\}^+$.[5] Isomerization, or dynamic processes, in single-crystal organometallics have been reported.[13]

Computationally the alternative form of [**3-NBA**][$\mathbf{BAr^F_4}$] was probed by rotating one complete cation within the unit cell and reoptimizing the structure (Scheme 2). This gives a local "parallel" structure analogous to that seen within [**2-NBA**]-[$\mathbf{BAr^F_4}$] and equivalent to the structure that would be formed if, upon hydrogenation, the NBD ligand in [**3-NBD**][$\mathbf{BAr^F_4}$] underwent rotation rather than the $\{Rh(L)_2\}^+$ cation. For [**3-NBA**][$\mathbf{BAr^F_4}$] the parallel structure is ca. 14 kcal/mol above the optimized "orthogonal" form. The parallel structure is therefore not viable thermodynamically, but it may be kinetically accessible, 14 kcal/mol representing a lower limit to the

DOI: 10.1021/acs.organomet.6b00645
Organometallics 2017, 36, 22−25

Scheme 2. Relative Energies for Parallel and Orthogonal Forms

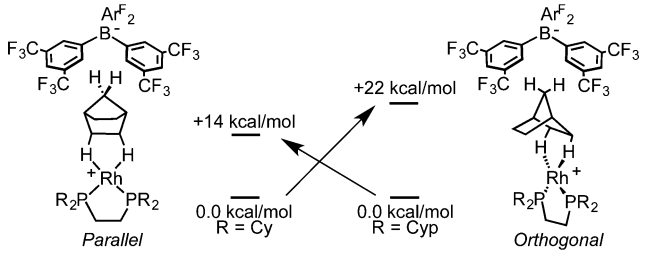

rearrangement barrier. For the more rigid [**2-NBA**][**BAr$^F_4$**] the experimentally observed[5] parallel structure lies 22 kcal/mol below the alternative orthogonal form.

The hydrogenation of microcrystalline [**3-NBD**][**BAr$^F_4$**] was studied by SSNMR. A $^{31}P\{^1H\}$ SSNMR spectrum (298 K) taken immediately after H_2 addition (10 min) shows complete consumption of [**3-NBD**][**BAr$^F_4$**], with two overlapping doublet signals observed (δ 109.2, $J_{RhP} \approx 189$ Hz; δ 108.1, $J_{RhP} \approx 188$ Hz), consistent with at least two crystallographically independent ^{31}P environments. Such a downfield shift and increase in the J_{RhP} value are consistent with the formation of a σ-alkane complex.[4,5,14] The $^{13}C\{^1H\}$ SSNMR spectrum lacks signals between δ 100 and 50 due to NBD.[9] We,[5,14] and others,[15] have previously used HETCOR SSNMR experiments to indirectly detect ^1H NMR signals in σ complexes, which in combination with computed chemical shifts has led to assignment of signals arising from σ-Rh···H−C interactions in σ-alkane complexes. The projected ^1H NMR spectrum from the $^{13}C/^1H$ FSLG-HETCOR SSNMR experiment conducted on freshly prepared [**3-NBA**][**BAr$^F_4$**] showed a broad high-field signal centered at ca. δ − 1.46 which correlates to a partially obscured ^{13}C signal at δ 25.[9] These chemical shifts are comparable to those reported for the σ-Rh···H−C interactions in [**2-NBA**][**BAr$^F_4$**].[5] An additional high-field signal at $\delta(^1H)$ −0.16 (cross peak $\delta(^{13}C)$ 40.5) is assigned to the ring-current-affected methylene bridge (C7) protons. A similar cross peak is observed for [**3-NBD**][**BAr$^F_4$**] ($\delta(^1H)$ − 1.74/$\delta(^{13}C)$ 69.3) in line with a similar orientation of the NBD ligand in the precursor.

Assignment of these NMR data on the basis of the computed ^{13}C and ^1H chemical shifts for [**3-NBA**][**BAr$^F_4$**] derived from the full extended solid-state structure (GIPAW method, PBE functional) is shown in Figure 3. Those for C1 and C2 (δ^{calc} ca.

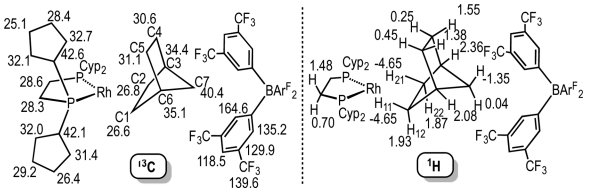

Figure 3. Computed ^{13}C and ^1H chemical shifts for [**3-NBA**][**BAr$^F_4$**] (GIPAW, PBE functional).

27) are in good agreement with experiment, while the associated H11 and H21 exhibit appreciable shielding (coincident at δ^{calc} −4.65) but are shifted more upfield than those in experiment (δ −1.46). The C7 position (δ^{calc} 40.4) matches experiment, and the ring current effect that shields the C7 hydrogens is also captured. The different values for H71 and H72 (δ^{calc} −1.35 and 0.04) reflect the asymmetry of the environment in the static structure. The observation experimentally of single resonances for H71/72 (δ −0.16) and H11/21 may therefore reflect a fluxional process occurring on the NMR time scale at 298 K that renders these sets of protons equivalent. Cooling to 158 K resulted in a broadened $^{31}P\{^1H\}$ SSNMR spectrum and a HETCOR in which signals due to the NBA ligand were too broad to be observed, consistent with a low-energy (∼7 kcal/mol) fluxional process occurring in the solid-state.[16] SSNMR calculations also reproduce well the change in J_{RhP} upon hydrogenation.[9]

Powdered crystalline [**3-NBA**][**BAr$^F_4$**] displayed stability intermediate between those of [**1-NBA**][**BAr$^F_4$**] (minutes) and [**2-NBA**][**BAr$^F_4$**] (months), as measured by $^{31}P\{^1H\}$ SSNMR spectroscopy. Signals for [**3-NBA**][**BAr$^F_4$**] were slowly (96 h) replaced by a broad signal centered at δ 84, assigned to zwitterionic [**3-BAr$^F_4$**], as confirmed by an independent synthesis.[9] Decomposition is effectively halted at 273 K.

Although we currently do not have a definitive explanation for the factors that control relative stabilities and the movements of NBA versus the metal fragment in the solid state, it may be noteworthy that the $PCyp_2$ groups offer a more curved exterior surface in comparison with the rigid/tall PCy_2 that could encourage $\{Rh(L_2)\}^+$ movement for the former in the relatively high symmetry cavity of $[BAr^F_4]^-$ anions (Figure 4). The delineation of such electronic and steric influences will

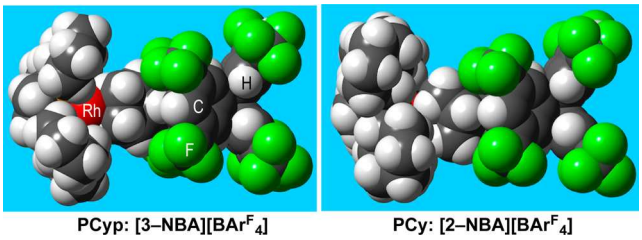

Figure 4. Space-filling representation (van der Waals radii) of [**3-NBA**][**BAr$^F_4$**] and [**2-NBA**][**BAr$^F_4$**][5] showing the relationship with a local $[BAr^F_4]^-$ anion.

be important in the continued development of the coordination chemistry and reactivity of σ-alkane complexes in the solid-state.

■ ASSOCIATED CONTENT

Supporting Information

The Supporting Information is available free of charge on the ACS Publications website at DOI: 10.1021/acs.organomet.6b00645.

Experimental and characterization details, including NMR spectroscopic data, X-ray crystallographic data, and computational details (PDF)

X-ray crystallographic data (CIF)

Cartesian coordinates for calculated structures (XYZ)

■ AUTHOR INFORMATION

Corresponding Authors

*E-mail for S.A.M.: s.a.macgregor@hw.ac.uk.

*E-mail for A.S.W.: andrew.weller@chem.ox.ac.uk.

Author Contributions

[§]These authors contributed equally to this work.

DOI: 10.1021/acs.organomet.6b00645
Organometallics 2017, 36, 22−25

Notes

The authors declare no competing financial interest.

■ ACKNOWLEDGMENTS

We acknowledge the EPSRC (A.S.W., S.A.M.; EP/M024210, EP/K035908, EP/K035681) for funding and Dr. Adrian Chaplin (University of Warwick) for useful discussions. This work used the ARCHER UK National Supercomputing Service (http://www.archer.ac.uk).

■ REFERENCES

(1) (a) Hall, C.; Perutz, R. N. *Chem. Rev.* **1996**, *96*, 3125−3146. (b) Labinger, J. A.; Bercaw, J. E. *Nature* **2002**, *417*, 507−514. (c) Jones, W. D. *Acc. Chem. Res.* **2003**, *36*, 140−146. (d) Young, R. D. *Chem. - Eur. J.* **2014**, *20*, 12704−12718.

(2) (a) McNamara, B. K.; Yeston, J. S.; Bergman, R. G.; Moore, C. B. *J. Am. Chem. Soc.* **1999**, *121*, 6437−6443. (b) Bernskoetter, W. H.; Schauer, C. K.; Goldberg, K. I.; Brookhart, M. *Science* **2009**, *326*, 553−556. (c) Torres, O.; Calladine, J. A.; Duckett, S. B.; George, M. W.; Perutz, R. N. *Chem. Sci.* **2015**, *6*, 418−424. (d) Yau, H. M.; McKay, A. I.; Hesse, H.; Xu, R.; He, M.; Holt, C. E.; Ball, G. E. *J. Am. Chem. Soc.* **2016**, *138*, 281−288.

(3) Pike, S. D.; Weller, A. S. *Philos. Trans. R. Soc., A* **2015**, *373*, 20140187.

(4) Pike, S. D.; Thompson, A. L.; Algarra, A. G.; Apperley, D. C.; Macgregor, S. A.; Weller, A. S. *Science* **2012**, *337*, 1648−1651.

(5) Pike, S. D.; Chadwick, F. M.; Rees, N. H.; Scott, M. P.; Weller, A. S.; Krämer, T.; Macgregor, S. A. *J. Am. Chem. Soc.* **2015**, *137*, 820−833.

(6) (a) Grellier, M.; Mason, S. A.; Albinati, A.; Capelli, S. C.; Rizzato, S.; Bijani, C.; Coppel, Y.; Sabo-Etienne, S. *Inorg. Chem.* **2013**, *52*, 7329−7337. (b) Douglas, T. M.; Brayshaw, S. K.; Dallanegra, R.; Kociok-Köhn, G.; Macgregor, S. A.; Moxham, G. L.; Weller, A. S.; Wondimagegn, T.; Vadivelu, P. *Chem. - Eur. J.* **2008**, *14*, 1004−1022. (c) Hackett, M.; Ibers, J. A.; Whitesides, G. M. *J. Am. Chem. Soc.* **1988**, *110*, 1436−1448.

(7) Betteridge, P. W.; Carruthers, J. R.; Cooper, R. I.; Prout, K.; Watkin, D. J. *J. Appl. Crystallogr.* **2003**, *36*, 1487.

(8) Wagner, T.; Schönleber, A. *Acta Crystallogr., Sect. B: Struct. Sci.* **2009**, *65*, 249−268.

(9) See the Supporting Information.

(10) Initial data collection at 150 K revealed a poorer structure with significantly larger displacement ellipsoids associated with the NBA. There is only a 0.9% change in unit cell volume between [**3-NBD**][**BAr$^{F}_{4}$**] and [**3-NBA**][**BAr$^{F}_{4}$**] at 150 K: V = 6142.10(16), 6197.3(3) Å^3, respectively.

(11) Lim, S. H.; Olmstead, M. M.; Balch, A. L. *Chem. Sci.* **2013**, *4*, 311−318.

(12) Pike, S. D.; Krämer, T.; Rees, N. H.; Macgregor, S. A.; Weller, A. S. *Organometallics* **2015**, *34*, 1487−1497.

(13) (a) Bogadi, R. S.; Levendis, D. C.; Coville, N. J. *J. Am. Chem. Soc.* **2002**, *124*, 1104−1110. (b) Edwards, A. J.; Burke, N. J.; Dobson, C. M.; Prout, K.; Heyes, S. J. *J. Am. Chem. Soc.* **1995**, *117*, 4637−4653.

(14) Chadwick, F. M.; Rees, N. H.; Weller, A. S.; Krämer, T.; Iannuzzi, M.; Macgregor, S. A. *Angew. Chem., Int. Ed.* **2016**, *55*, 3677−3681.

(15) Smart, K. A.; Grellier, M.; Coppel, Y.; Vendier, L.; Mason, S. A.; Capelli, S. C.; Albinati, A.; Montiel-Palma, V.; Munoz-Hernandez, M. A.; Sabo-Etienne, S. *Inorg. Chem.* **2014**, *53*, 1156−1165.

(16) Chadwick, F. M.; Krämer, T.; Gutmann, T.; Rees, N. H.; Thompson, A. L.; Edwards, A. J.; Buntkowsky, G.; Macgregor, S. A.; Weller, A. S. *J. Am. Chem. Soc.* **2016**, DOI: 10.1021/jacs.6b07968.

DOI: 10.1021/acs.organomet.6b00645
Organometallics 2017, 36, 22−25